

Tunneling spectroscopy of a quantum dot through a single impurity

Erik Lind,* Boel Gustafson,† Ines Pietzonka,‡ and Lars-Erik Wernersson§
Solid State Physics/Nanometer Structure Consortium, Box 118, S-22100 Lund, Sweden
 (Received 17 March 2003; published 30 July 2003)

A single impurity inside a resonant tunneling diode is used to perform tunneling spectroscopy on an adjacent electrostatically defined vertical quantum dot. This results in tunneling between two zero-dimensional systems, measured as a set of sharp peaks in the current-voltage spectrum for finite bias. Magnetic-field-dependent measurements show that the angular momentum of the tunneling electrons is conserved during the tunneling process. Both ground and excited states are probed. The effect of temperature is also investigated, exhibiting a peak broadening that is smaller than 1 kT.

DOI: 10.1103/PhysRevB.68.033312

PACS number(s): 73.21.La, 73.40.Gk, 73.20.Hb

Tunneling spectroscopy is an important tool to investigate the electronic structure of low-dimensional systems. Studies have been made on such systems as quantum dots in different geometries¹ and single impurities.² Both types of structures have also been used to investigate properties of the surrounding contacts, including studies of local density-of-states (LDOS) fluctuations,³ Landau-level formation,⁴ and Fermi edge singularities.⁵ Consequently, specially designed low-dimensional emitter structures⁶ must be used to avoid effects originating from the emitter contact.

In this paper, we use a single impurity to perform tunneling spectroscopy on an adjacent electrostatically defined quantum dot. Since the lateral confinement of the impurity is much stronger than the relatively weak confinement of the quantum dot, the impurity essentially is unaffected by changes in the gate voltage or by a B field applied parallel to the current. In this sense, the impurity acts as an ideal emitter for tunneling spectroscopy. This zero-dimensional–zero-dimensional (0D-0D) tunneling process results in sharp peaks in the current-voltage characteristics (I - V) for finite biases. The quantum dots states show clear shifts with an applied magnetic field. These shifts fit with the Darwin-Fock model of a 2D harmonic oscillator in a magnetic field, assuming the conservation of the angular quantum number during the tunneling process. The effect of the gate in our transistor structure is more complex, with shifts probably due to charging effects. We performed temperature-dependent measurements, which further support the 0D-0D tunneling model. The data show a broadening of the peaks that is smaller than 1 kT, possibly due to coupling to acoustic phonons. When combined, these data give a clear picture of the tunneling coupling between the impurity and the dot, which highlights the effects of momentum conservation and the complicated interplay between charging and confinement effects in the dot.

The investigated sample is a GaAs-based resonant tunneling transistor consisting of a metallic tungsten gate embedded between two resonant tunneling diodes (RTD's). A cross section of the device is sketched in the inset of Fig. 1. The diodes have 5-nm-thick GaAs_{0.3}P_{0.7} barriers and 12-nm-thick GaAs wells surrounded by 20-nm-thick undoped spacer layers. The rest of the structure has a doping level of $2 \times 10^{17} \text{ cm}^{-3}$. All layers are grown by metal-organic vapor phase epitaxy (MOVPE) at optimized conditions.⁷ The gate

consists of 90- and 20-nm-thick wires separated by 100 nm. Overlapping Schottky depletion regions around the wires form an insulating area around the metal wires and direct the current through a designed $0.5 \times 0.5\text{-}\mu\text{m}^2$ large square opening in the middle of the grating. The details of the fabrication process are published elsewhere.⁸

From comparisons with current densities in reference diodes, we estimate that the upper RTD has a large conducting area, on the order of $130 \times 130 \text{ nm}^2$ at $V_g = 0 \text{ V}$, whereas the lower RTD has a conducting area as low as $50 \times 50 \text{ nm}^2$.⁸ From the depletion around the metal gate and the barriers of the two RTD's, a quantum dot is created between the two RTD's, as indicated in the inset of Fig. 1. From the background doping in the MOVPE we will have one or a few donor atoms in the active region of the upper RTD. An impurity inside a quantum well is known to create a resonant state slightly below the first bound state of the quantum well, with a binding energy on the order of 10 meV.⁹

The operation of the device is based on current conservation between the two RTD's with different areas. For large values of the collector bias, peaks originating from 3D-2D tunneling through the bound state of each individual RTD are observed. The operation of the device is described in Ref. 8. In this paper we focus our attention on a set of fine features observed prior to the main current onset, as shown in Fig. 2. Similar features were observed in other devices with openings of up to $1 \times 1 \mu\text{m}^2$. In our proposed model, the peaks

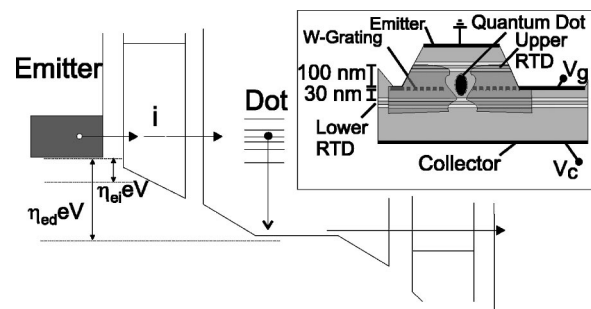


FIG. 1. Conduction-band profile of the device shows how the impurity state probes the dot states. The inset shows a schematic overview of the structure, indicating the depleted region around the tungsten wires. Note the formation of a quantum dot in between the two RTD's.

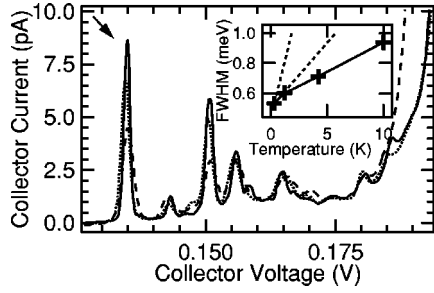


FIG. 2. I - V characteristics measured at $B=0$ T and $V_g = -50$ mV for different temperatures. The solid line is for 0.3, the dotted 4.2, and the dashed 10 K. For $V_c < 0.12$ the current is less than 0.1 pA and structureless. The inset shows the full width at half maximum of the peak denoted by an arrow, marked with crosses. The solid line is introduced to guide the eye. For reference, the dotted lines show 3.5 and 1 kT.

originate from a transport process schematically illustrated in Fig. 1. An electron tunnels through the lowest impurity state inside the upper quantum well, and then tunnels into the quantum dot between the two RTD's. By applying a positive bias V_c to the collector contact the energy of the dot states is lowered relative to the emitter Fermi level: $E_{\text{dot}} = E_{\text{dot}}(B, V_g) - eV_c \eta_{\text{ed}}$, where $E_{\text{dot}}(B, V_g)$ is the energy at zero bias, V_g is the applied gate voltage, B is the applied magnetic field, and η_{ed} is the voltage-to-energy conversion coefficient between the dot and emitter. The impurity state behaves in a similar way: $E_i = E_i(V_g) - eV_c \eta_{\text{ei}}$, where η_{ei} is the corresponding conversion coefficient for the impurity state. Due to conservation of energy, we only get a tunneling current when

$$V_c = \frac{E_{\text{dot}}(B, V_g) - E_i(V_g)}{e(\eta_{\text{ed}} - \eta_i)} \quad (1)$$

and $E_i < E_f$. E_f is the Fermi energy on in the emitter contact. By measuring shifts in V_c , we can directly detect how the dot states change in comparison with the impurity. The fulfillment of Eq. (1) results in a series of sharp peaks in the current-voltage (I - V) characteristics, as different dot states align with the impurity state, as indicated in Fig. 1. In addition, tunneling paths through the lower RTD are considered. However, due to the smaller effective conducting area of the lower RTD compared with the upper one, modeling has shown that a larger part of the applied bias falls over the lower RTD (Ref. 8) and consequently brings down the bound state of the RTD as indicated in Fig. 1. Thus there are always tunneling paths out through the device. The lower RTD has also most likely 0D characteristics due to the close proximity to the gate. This might add some additional structure to the data, however, we have not been able to relate any characteristics in the data due to lateral quantization in the lower RTD.

Figure 2 shows the I - V characteristics measured for $V_g = -50$ mV for three different temperatures. The set of very sharp peaks in the collector current (I_c) is observed for collector biases (V_c) between 0.1 and 0.2 V. Such peaks in the

I - V are attributed to 0D-0D tunneling,¹⁰ and a similar structure has previously been reported for stacked quantum dot systems.⁶

We then investigate the effect of the gate voltage. Figure 3 shows a color plot of the I - V as a function of V_g . For the used values of V_g , the gate current remained below 100 fA and showed no significant structure. Most peaks have a slight shift toward lower voltages with increasing negative gate bias during a small range of applied gate bias. More pronounced are the sharp, large shifts indicated by green lines in Fig. 3. The regions formed between the lines are denoted as $a, a+1$. At each such shift, the entire set of peaks are shifted toward higher V_c when going from $a+(n)$ to $a+(n+1)$, whereas the voltage separation between the peaks as well as the number of peaks remain essentially constant. This indicates that the dot states are suddenly shifted towards higher voltages compared with the emitter state. With $(\eta_{\text{ed}} - \eta_i) \approx 0.4$ (extracted for magnetic-field measurements, as shown below), the shifts correspond to about 1.5 up to 6 meV. The probable origin is Coulomb charging effects inside the dot or the lower RTD, but we cannot rule out effects related to depletion of individual donor atoms inside or near the dot. We estimate the capacitance of the dot with the self-capacitance of a sphere, $C_{\text{self}} = 2\pi\epsilon_r\epsilon_0 d_{\text{eff}}$, which for $d_{\text{eff}} = 60$ nm gives roughly $C_{\text{self}} \approx 40$ aF. This corresponds to a charging energy of $E_c = e^2/C_{\text{self}} \approx 4$ meV. This is of the same order of magnitude of the measured shifts, considering the rough estimate of the charging energy. The slopes of the green lines between the different regions are most likely due to self-gating effects.

Next we apply a magnetic field parallel to the current. The data are shown as a color plot in Fig. 4. The magnetic field shifts all peaks to higher collector bias, with essentially three different slopes, $\partial V_c / \partial B$, in the high-field region. From Eq. (1) we conclude that this implies that the dot states monotonously move towards higher energies with increasing field, compared with the emitter states. To explain the positive shifts, we assume that the emitter state is a single impurity inside the upper RTD, and that the observed shift originates from an energy shift in the dot state. The diamagnetic shift of an impurity-induced state is on the order of 1 meV for our used magnetic-field strength,³ which is considerably smaller than our measured shift of 5–6 meV, as we show below. The lateral confining potential is further approximated to be parabolic. For a 2D harmonic oscillator in a magnetic field (neglecting spin), the eigenstates are the so-called Darwin-Fock states,¹¹ with eigenenergies

$$E_{n,m_d} = (2n + |m_d| + 1)\hbar \sqrt{\omega_0^2 + \frac{\omega_c^2}{4}} + \frac{1}{2}\hbar\omega_c m_d, \quad (2)$$

where $\omega_c = eB/m^*$, $\hbar\omega_0$ is the electrostatic confinement energy, m_d is the angular momentum quantum number, n is the main quantum number, and m^* is the effective mass of GaAs. Any states with a negative value of m_d will move towards lower energies for low magnetic fields ($\hbar\omega_c \ll \hbar\omega_0$) compared with the confinement energy. Since we do not observe any negative shifts in the peak voltages, all observed dot states must have $m_d \geq 0$. Most peaks are believed

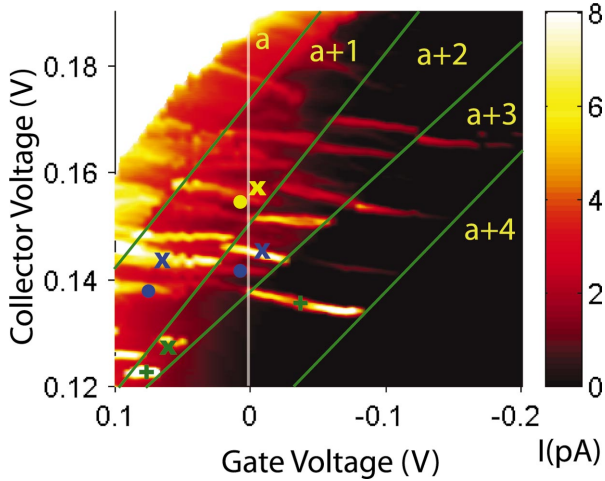


FIG. 3. (Color) Color plot of the current vs V_c and V_g , for $B = 0$ T. The green lines indicated discrete shifts between the different regions. The same method of identification of the peaks as in Fig. 4 below has been used here to mark the different families of peaks.

to come from electrons tunneling through the ground state of the hydrogenic impurity, which, like an s -like state, has an angular momentum of $m_i = 0$.⁹ If we assume radial symmetry of our dot,¹² the wave function of the dot is as follows: $\Psi(r, \theta, z) = e^{im_d\theta} / \sqrt{2\pi} \psi(r, z)$. Using the transfer Hamiltonian method to describe the tunneling process, one obtains the selection rule that $m_i = m_d$.¹³ For quantum dots that do not show radial symmetry, m_d is not a good quantum number any longer and the selection rule does not hold rigorously. However, for weak deviations from the radial symmetry the quantum dot wave functions are virtually radial symmetric, and the impurity states couple only strongly to dot states with angular wave functions, similar to the m_i impurity state.

Because the impurity state has $m_i = 0$, we can only tunnel to dot states with $m_d = 0$. Using this criteria, Eq. (2) simplifies to

$$E_{n,0} = (2n+1)\hbar \sqrt{\omega_0^2 + \frac{\omega_c^2}{4}}. \quad (3)$$

By combining Eqs. (1) and (3) an expression for the peak voltages as a function of the B field can be obtained. The different symbols (\times, \cdot) in Fig. 4 are fittings of Eqs. (1) and (3) for $n=0-2$ with $\hbar\omega_0 = 2.4$ and 2.6 meV, respectively, and with $(\eta_{ed} - \eta_i) = 0.36$ and 0.37 . Good fittings are thus achieved for both ground and excited states of the quantum dot. The discrete shifts of each fit at certain B fields are due to effects originating from the gate, as explained above. For the peak fitted with (+), only the ground state could be observed with $\hbar\omega_0 = 2.0$ meV and $(\eta_{ed} - \eta_i) = 0.36$. The energy separation between the (\times) and the (\cdot) ground states is roughly 1.5 meV. The origin of the various ground states is most likely due to different vertical states or the same vertical state with a different number of electrons in the dot. Due to the complicated potential structure of the dot, the various ground states might not all have the same lateral confining

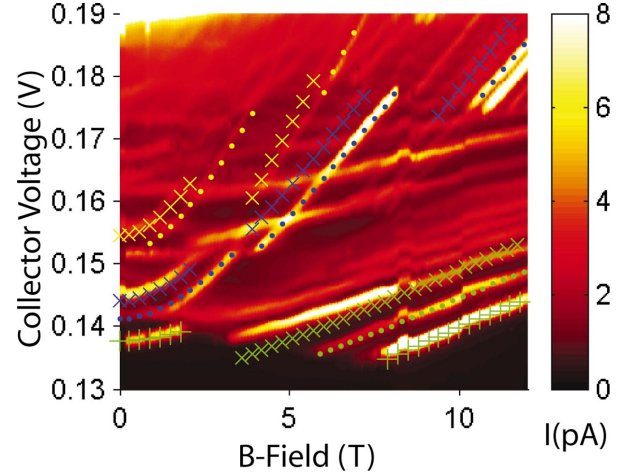


FIG. 4. (Color) Color plot of the B -field dependence on the I - V characteristics, measured at $V_g = 0$ V. Three fittings to Eq. (3) have been done, represented by dots (\cdot), crosses (\times), and plus signs ($+$). Each marked peak with the same symbol belongs to the same vertical state, but with different lateral quantum numbers, which are color coded as follows: Green signs correspond to $n=0$ states, blue to $n=1$ states, and yellow to $n=2$ states. For the peak fitted with (+), only a fitting of the ground state could be obtained.

energies. From the classical turning points, the diameter of the dot state can be estimated to be $d_{\text{dot}} = 2\sqrt{2\hbar/m^* \omega_0} \approx 60$ nm. Similar fittings can be done for a majority of the other peaks as well, with slightly different values of $\hbar\omega_0$ and $(\eta_{ed} - \eta_i)$. For most peaks, however, only the ground state is observed.

In the B -field-dependent data in Fig. 4, there are peaks appearing and disappearing at certain values of the applied B field. For example, the (+) peak is visible from 0 up to 2 T, and then reappears at 8 T. To be able to explain this anomalous behavior, we need to consider the effect of the gate as well. As explained above, for certain applied collector voltages the entire set of curves is shifted in respect to each other. In the fittings of the B -field data in Fig. 4 these shifts have been taken into account. The white line in Fig. 3 indicates that $V_g = 0$ V, at which the magnetic-field-dependent measurement was made. At $B = 0$ T, the line intercepts the $n=1$ (\times) and (\cdot) peaks in the ($a+2$) region, and the $n=0$ (+) peak in the ($a+3$) region, which are visible in the low-field region of Fig. 4. On the other hand, the ground state of, for example, the $n=0$ (\times) peak in the ($a+2$) region is not intercepted, and it is thus not visible in Fig. 4 for low values of magnetic fields.

In spite of the simple model used to generate the fittings, very good agreement with the measured data is obtained. This verifies the model of coupling between a impurity and a quantum dot as well as conservation of angular momentum.

We finally turn to the temperature dependence of the I - V characteristics. As shown in Fig. 2 essentially all curves are smeared out with increasing temperature, however, the effect is relatively weak, which rules out broadening related to smearing of the Fermi edge. Peaks are visible up to roughly 20–30 K, at which point they disappear in the background current. The inset of Fig. 2 depicts the full width at half

maximum (FWHM) of the peak marked with an arrow in Fig. 2. The peak has an intrinsic width of roughly 0.5 meV if extrapolated to 0 K. Calculations of the FWHM of a donor-induced state inside a quantum well gives that the energy width of the state is on the order of 0–1 meV, depending on the quantum well thickness and the position of the donor atom inside the quantum well.¹⁴ This agrees with our measured width, which indicates that the observed width originates from the impurity-induced state. For a state probing the Fermi edge, the expected peak FWHM dependency of the temperature is 3.5 kT,¹⁵ which is much larger than our measured broadening, as shown in the inset. Our measured broadening could instead originate from inelastic tunneling via acoustic phonons.¹⁶

In summary, we have investigated the coupling between a single impurity and an electrostatically formed quantum dot, by using a stacked resonant tunneling transistor structure. The resulting I - V characteristics show a set of very sharp

peaks, which is expected from tunneling between two 0D systems. The magnetic-field dependence was fitted with a Darwin-Fock spectrum, which shows that the angular momentum is conserved during the tunneling process. The effect of the gate voltage is more unclear, but, in combination with the magnetic-field-dependent data, it indicates the presence of an emitter that consists of a single impurity atom. The effect of the B field on the current is complicated by self-gating effects, which induce shifts probably originating from charging effects inside the dot. The temperature dependence also supports the 0D-0D tunneling model, with a peak broadening smaller than 1 kT.

The authors would like to thank Professor R. Haug and Dr. U. Zeitler for valuable discussions and Professor L. Samuelson for his encouragement and support. This work was supported by SSF, the Swedish Research Council, and a Marie Curie grant.

*Email address: Erik.Lind@ftf.lth.se

[†]Present address: Ericsson Mobile Platforms, S-22183 Lund, Sweden.

[‡]Present address: OSRAM Opto Semiconductors GmbH, D-93049 Regensburg, Germany.

[§]Present address: Department of Electrical Engineering, University of Notre Dame, Notre Dame, IN 46556.

¹L. P. Kouwenhoven, D. G. Austing, and S. Tarucha, Rep. Prog. Phys. **64**, 701 (2001).

²M. R. Deshpande, J. W. Sleight, M. A. Reed, R. G. Wheeler, and R. J. Matyi, Phys. Rev. Lett. **76**, 1328 (1996).

³T. Schmidt, R. J. Haug, V. I. Fal'ko, K. v. Klitzing, A. Förster, and H. Lüth, Phys. Rev. Lett. **78**, 1540 (1997).

⁴P. C. Main, A. S. G. Thornton, R. J. A. Hill, S. T. Stoddart, T. Ihn, L. Eaves, K. A. Benedict, and M. Henini, Phys. Rev. Lett. **84**, 729 (2000).

⁵A. K. Geim, P. C. Main, N. La Scala Jr., L. Eaves, T. J. Foster, P. H. Beton, J. W. Sakai, F. W. Sheard, M. Henini, G. Hill, and M. A. Pate, Phys. Rev. Lett. **72**, 2061 (1994).

⁶T. Bryllert, M. Borgström, T. Sass, B. Gustafson, L. Landin, L.-E. Wernersson, Werner Seifert, and L. Samuelson, Appl. Phys. Lett. **80**, 2681 (2002).

⁷L.-E. Wernersson, K. Georgsson, A. Gustafsson, A. Löfgren, L.

Montelius, N. Nilsson, H. Pettersson, W. Seifert, L. Samuelson, and J.-O. Malm, J. Vac. Sci. Technol. B **20**, 580 (2002).

⁸E. Lind, I. Pietzonka, P. Lindström, W. Seifert, and L.-E. Wernersson, Appl. Phys. Lett. **81**, 1905 (2002).

⁹R. L. Greene and K. K. Bajaj, Solid State Commun. **45**, 825 (1983).

¹⁰G. W. Bryant, Phys. Rev. B **44**, 3064 (1991).

¹¹V. Fock, Z. Phys. **47**, 446 (1928).

¹²The opening in the tungsten gate is nominally square, however, due to the Schottky depletion, the central part of the dot is essentially circular [P. Matagne and J. P. Leburton, Phys. Rev. B **65**, 155311 (2002)].

¹³B. Jouault, M. Boero, G. Faini, and J. C. Inkson, Phys. Rev. B **59**, 4966 (1999).

¹⁴A. Blom, M. A. Odnoblyudov, I. N. Yassievich, and K.-A. Chao, Phys. Status Solidi B **235**, 85 (2003).

¹⁵M. R. Deshpande, E. S. Hornbeck, P. Kozodoy, N. H. Dekker, J. W. Sleight, M. A. Reed, C. L. Fernando, and W. R. Frensley, Semicond. Sci. Technol. **9**, 1919 (1994).

¹⁶T. Fujisawa, T. H. Oosterkamp, W. G. van der Wiel, B. W. Broer, R. Aguado, S. Tarucha, and L. P. Kouwenhoven, Science **282**, 932 (1998).